International Journal of Multidisciplinary Studies and Innovative Technologies

e-ISSN: 2602-4888
dergipark.org.tr/en/pub/ijmsit
Research Article

2025, 9 (1), 47-52
DOI: 10.36287/ijmsit.9.1.7
Received: April 25, 2025; Accepted: June 27, 2025

Lateral Resolution Enhancement of Ultrasound Images via Auto-Encoder Network

Mahsa Mikaeili[1*], Hasan Şakir Bilge [2,3]

[1*]*Mechatronic Engineering/İstanbul Okan University, İstanbul, Turkey (mahsa.mikaeili@okan.edu.tr) (ORCID: 0000-0002-8072-4353)*
[2]*Electrical-Electronics Engineering/Gazi University Engineering Faculty, Ankara, Turkey (bilge@gazi.edu.tr) (ORCID: 0000-0002-4945-0884)*
[3]*Biomedical Calibration and Research Center/Gazi University, Ankara, Turkey*

Abstract – Ultrasound imaging is widely used for medical diagnostics, but its resolution is inherently constrained by factors such as wavelength, focal length, scan line density, and frame rate. A fundamental trade-off exists between lateral and temporal resolution, where increasing scan line density enhances spatial detail at the expense of reduced frame rates. This study explores the potential of deep learning, specifically an AutoEncoder-based approach, to enhance lateral resolution without sacrificing temporal resolution. The performance of the AutoEncoder is evaluated against traditional interpolation methods, including nearest, linear, and spline interpolation, using structural similarity (SSIM), peak signal-to-noise ratio (PSNR), multi-scale SSIM (MS-SSIM), and feature similarity (FSIM) metrics. The results demonstrate that the AutoEncoder outperforms interpolation methods, achieving the highest SSIM and FSIM, indicating superior structural preservation and feature retention. Additionally, the RF signal analysis shows that while the AutoEncoder maintains the overall waveform structure, minor amplitude and phase deviations exist. These findings suggest that deep learning-based super-resolution can effectively enhance lateral resolution while minimizing traditional resolution trade-offs.

Keywords *– Ultrasound Imaging, Resolution Enhancement, lateral resolution, Deep Learning, Interpolation.*

Citation: Mikaeili, M., Bilge, H, Ş. (2025). Lateral Resolution Enhancement of Ultrasound Images via Auto-Encoder Network. International Journal of Multidisciplinary Studies and Innovative Technologies, 9(1): 47-52.

I. INTRODUCTION

Ultrasound imaging systems (US) are one of the standard imaging modalities in medicine, and they have multiple advantages over other imaging modalities. From the point of view of patient safety, US systems lack ionizing radiation and are also non-invasive. In addition, these systems are portable and allow patient monitoring at the bedside. The most important advantage of the US is providing real-time images [1]. These advantages enable this medical device to monitor a region of interest (ROI) during biopsy or apply it intraoperatively with a combination of other imaging during surgery.

However, this imaging modality has some drawbacks arising from its inherent attributes. First of all, this imaging modality is prone to speckle noise. In addition, extending their resolution cells in an elevational distance, in turn, created an overlap between consecutive frames and caused artifacts in US images, and finally, US serves images with low resolution compared to other biomedical imaging modalities [2,3].

Generally, US image resolution is affected by different factors such as wavelength, focal length, number of scan lines, frame rates, etc. There is an inherent trade-off between lateral and temporal resolution in ultrasound imaging. Increasing the number of scan lines enhances lateral resolution by reducing the spacing between adjacent beams, thereby improving spatial detail. However, this comes at the expense of temporal resolution, as acquiring additional scan lines requires more time, reducing the frame rate. Conversely, reducing the number of scan lines increases the frame rate, thereby improving temporal resolution but at the cost of degraded lateral resolution due to larger beam spacing.

Different studies applied different approaches to tackle this issue and increase ultrasound resolution. In [4], the authors classified these approaches into three methods. The first group relied on images. These studies [5-8] focused on increasing the resolution of B-mode US images by applying super-resolution methods. These methods apply to the final stage of US image creation. According to [4], there are also two other classes; however, these classes rely on RF data rather than US images and attempt to reconstruct US images with high resolution, either by employing pre-beamformed RF data or post-beamformed RF data.

Among the methods that rely on post-beamformed methods are [9,10]. In [9], a deep neural network (DNN) was proposed that integrates sparse regularization into its loss function to produce high-quality images with reduced computation time. Similarly, [10] introduced a model that enhances delay-and-sum (DAS) beamforming by generating pixel-wise weights from single-angle (0°) plane wave data, achieving improved image quality over traditional methods.

Besides studies that rely on post-beamformed data, some studies, such as [11-18], rely on pre-beamformed data. In [11], the authors adapted MobileNetV2 to emulate Minimum Variance Beamforming (MVB), achieving comparable image

quality with significantly reduced reconstruction time. Similarly, [12] utilized a U-Net-inspired architecture with strided convolutions to reconstruct images from raw channel data acquired via single-angle plane wave insonification, producing results visually similar to conventional delay-and-sum methods. In [13], an autoencoder-based model, also inspired by U-Net, was proposed for beamforming using RF data from a single plane wave transmission.

In [14], a fully convolutional network trained on simulated channel data and echogenicity maps was used to reduce speckle noise in B-mode images by processing 16 sub-aperture RF signals. In [15], a conditional GAN (cGAN) was proposed to directly convert raw RF channel data into B-mode images, effectively bypassing conventional beamforming.

In [16], a fully convolutional neural network was proposed to replace traditional beamforming by framing ultrasound image reconstruction as a segmentation task applied directly to pre-beamformed RF data. Similarly, [17] introduced a deep learning approach to balance image quality and clinical usability, demonstrating that their model enhances reconstruction quality and acquisition frequency, supporting real-time ultrasound applications. In [18], a tight frame U-Net architecture was employed to enhance the Point Spread Function (PSF) in plane-wave imaging. The method reconstructs high-quality Tissue Reflectivity Functions (TRFs) from pre-beamformed RF data using a single plane-wave transmission, modeling the TRF as an isotropic 2D Gaussian kernel convolved with a cosine function.

Another investigated work is [19]. The authors propose a deep learning approach that unifies RF data from different angles by learning a linear transformation to a standard 0° reference. A two-stage neural network is introduced: PixelNet, a fully convolutional network that optimizes pixel-wise weights for enhancing DAS images, and a cGAN for further image refinement.

All of the investigated studies demonstrate the growing impact of deep learning in ultrasound image reconstruction, particularly for ultrafast plane wave imaging. Research has explored post-beamformed and pre-beamformed RF data to enhance image quality, reduce computational complexity, and improve real-time usability [4]. One critical limitation of ultrafast plane wave imaging is the trade-off between frame rate and lateral resolution. Many deep learning-based approaches have been designed to reconstruct high-quality images from limited data, often relying on a single insonification angle. However, despite improving resolution and contrast using these methods, lateral resolution remains a significant challenge.

As previously mentioned, lateral resolution in ultrasound imaging is directly affected by the number of scan lines used to form an image. A higher number of scan lines leads to better spatial sampling, reducing artifacts and improving the visualization of fine structures. Many reviewed studies focus on enhancing resolution using deep learning, but their effectiveness can be further improved by increasing the number of scan lines. This would allow neural networks to exploit spatial information better, leading to superior image quality, improved diagnostic accuracy, and enhanced clinical applicability.

Despite these advancements, most existing deep learning approaches operate within the constraints of fixed spatial sampling or apply enhancement in the image domain without explicitly addressing scan line density. Our proposed method introduces an Autoencoder-based framework that directly targets the lateral resolution by learning to synthesize high-density lateral information from low-density RF inputs. This is achieved by training the Autoencoder to map low-resolution input representations (fewer scan lines) to their high-resolution counterparts, effectively learning a non-linear upsampling function in the RF or image domain. Unlike traditional interpolation techniques, the Autoencoder captures contextual and structural priors across the lateral dimension. This enables it to reconstruct anatomically coherent details with reduced artifacts and improved Point Spread Function (PSF) characteristics. By operating in this learned feature space, the network leverages spatial dependencies that are typically underutilized in classical beamforming, thus pushing the boundaries of lateral resolution enhancement in ultrafast ultrasound imaging.

Therefore, this study aims to increase the number of scan lines or lateral resolution by employing an Autoencoder and, consequently, improve the lateral resolution of US images. The remainder of this paper is organized as follows. Section II discusses the applied methods and materials, and the results and discussion are presented in Sections III and IV, respectively.

II. Materials and Methods

This section presents the theoretical background of AutoEncoder and the data acquisition process.

A. Applied Network

In this study, an AutoEncoder model is utilized to enhance the lateral resolution of US images. An Autoencoder is a neural network designed for unsupervised learning, primarily used for dimensionality reduction, feature extraction, and image reconstruction. It consists of two main components: an encoder and a decoder. The encoder compresses the input data into a lower-dimensional representation, often called the latent space or bottleneck, capturing the essential features while discarding noise and redundant information. The decoder then reconstructs the original input from this compressed representation, aiming to minimize the reconstruction loss.

In general, super-resolution autoencoders are designed with skip connections, upsampling layers, and transposed convolutions to enhance fine details and improve the image quality.

Since this study aims to enhance the lateral resolution of US images, our utilized network consists of 18 layers, including convolutional, pooling, dropout, upsampling, and element-wise addition layers. The encoder comprises five convolutional layers with ReLU activation, progressively increasing the number of filters from 64 to 256 while applying MaxPooling2D in the lateral dimension only to reduce width while preserving axial resolution. A dropout layer (0.3) is applied at the bottleneck to prevent overfitting. The decoder then symmetrically up-samples the lateral dimension using.

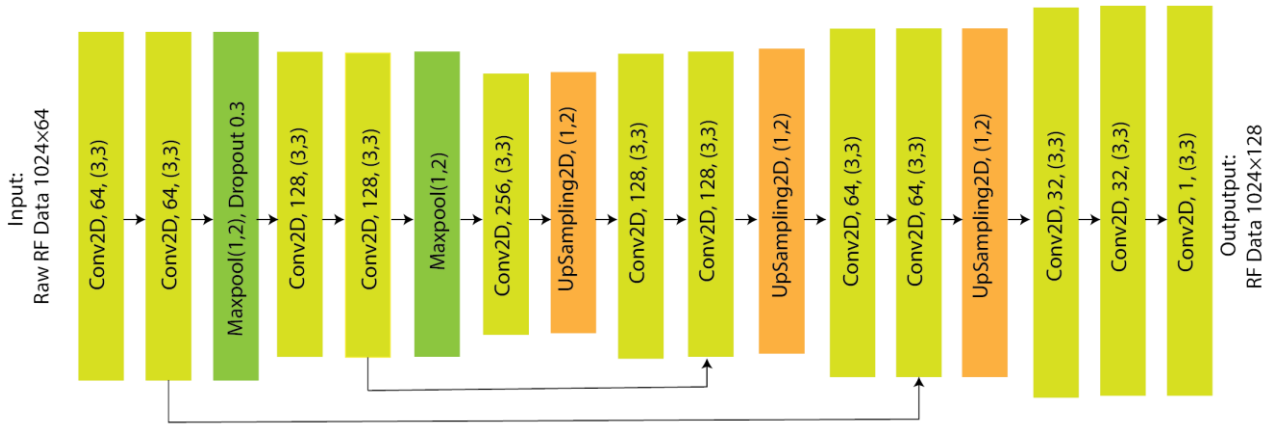

Fig.1. AutoEncoder block diagram

Table1. Summary of network layers.

Layer (Type)	Output Shape	Param #	Connected to
input_1 (InputLayer)	(None, 1024, 64, 1)	0	
conv2d (Conv2D)	(None, 1024, 64, 64)	640	input_1[0][0]
conv2d_1 (Conv2D)	(None, 1024, 64, 64)	36,928	conv2d[0][0]
max_pooling2d (MaxPooling2D)	(None, 1024, 32, 64)	0	conv2d_1[0][0]
dropout (Dropout)	(None, 1024, 32, 64)	0	max_pooling2d[0][0]
conv2d_2 (Conv2D)	(None, 1024, 32, 128)	73,856	dropout[0][0]
conv2d_3 (Conv2D)	(None, 1024, 32, 128)	147,584	conv2d_2[0][0]
max_pooling2d_1 (MaxPooling2D)	(None, 1024, 16, 128)	0	conv2d_3[0][0]
conv2d_4 (Conv2D)	(None, 1024, 16, 256)	295,168	max_pooling2d_1[0][0]
up_sampling2d (UpSampling2D)	(None, 1024, 32, 256)	0	conv2d_4[0][0]
conv2d_5 (Conv2D)	(None, 1024, 32, 128)	295,040	up_sampling2d[0][0]
conv2d_6 (Conv2D)	(None, 1024, 32, 128)	147,584	conv2d_5[0][0]
add (Add)	(None, 1024, 32, 128)	0	conv2d_3[0][0], conv2d_6[0][0]
up_sampling2d_1 (UpSampling2D)	(None, 1024, 64, 128)	0	add[0][0]
conv2d_7 (Conv2D)	(None, 1024, 64, 64)	73,792	up_sampling2d_1[0][0]
conv2d_8 (Conv2D)	(None, 1024, 64, 64)	36,928	conv2d_7[0][0]
add_1 (Add)	(None, 1024, 64, 64)	0	conv2d_8[0][0], conv2d_1[0][0]
up_sampling2d_2 (UpSampling2D)	(None, 1024, 128, 64)	0	add_1[0][0]
conv2d_9 (Conv2D)	(None, 1024, 128, 32)	18,464	up_sampling2d_2[0][0]
conv2d_10 (Conv2D)	(None, 1024, 128, 32)	9,248	conv2d_9[0][0]
conv2d_11 (Conv2D)	(None, 1024, 128, 1)	289	conv2d_10[0][0]

Three UpSampling2D layers and four additional convolutional layers to reconstruct high-resolution features. The network integrates two skip connections (add layers) to retain spatial information lost during down-sampling. The final output layer is a single-channel convolutional layer with ReLU activation, ensuring positive pixel values. The model is compiled with the Adam optimizer, mean squared error (MSE) loss function, and a learning rate of 0.000001. During training, 50 epochs and a batch size of 2 were used. Additionally, early stopping was not performed. Fig.1 and Table.1 show a block diagram of the applied network and its parameters, respectively.

B. Data Acquisition

To evaluate our method and perform training, synthetic ultrasound (US) images were generated using Field II [20] and MATLAB. The US data simulation was conducted for two scan line configurations: 64 and 128. The dataset with 64 RF scan lines was used as the network input, while the dataset with 128 RF scan lines served as the ground truth during the training and testing phases. A total of 220 point reflectors were simulated, with varying numbers of reflectors per sample, ranging from 1 to 4. Additionally, the simulations were performed without apodization. Out of the total dataset, 205

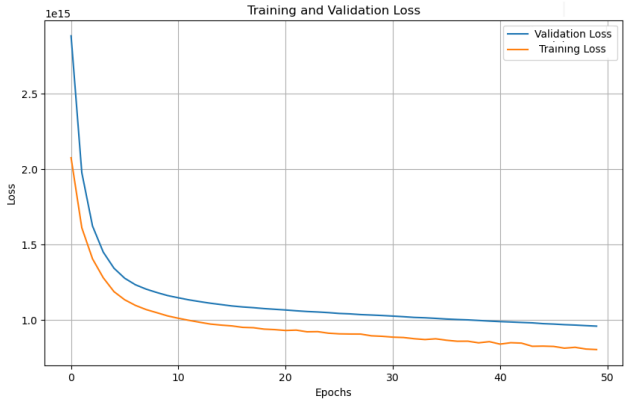

Fig.2. Training loss of AutoEncoder for enhancing lateral resolution.

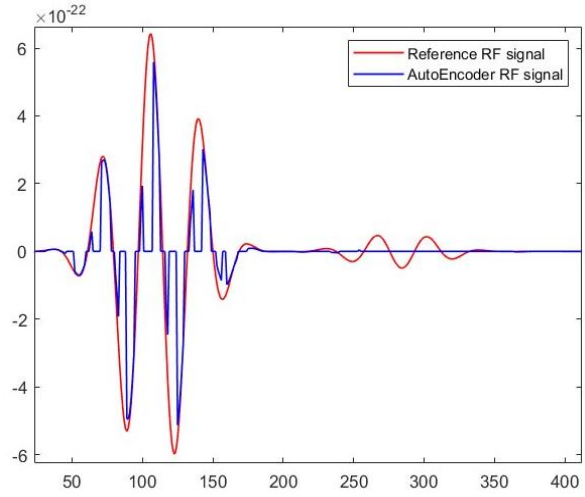

Fig.3. Comparison of ground truth signal with the reconstructed signal by using AutoEncoder.

samples were used for training, while the remaining data were reserved for testing. Out of the 205 training samples, 40 were reserved for validation purposes. The experiments were performed on an Intel i7 8th-generation processor unit (4 GHz with 32 GB RAM) and an NVIDIA GeForce GTX. All the software codes were built using TensorFlow.

III. RESULTS

This study aims to enhance the lateral resolution of ultrasound images by employing the AutoEncoder model. Our inputs are raw RF data (64 scan lines). Also, the network's output is RF data with a higher number of scan lines (128 scan lines). Then, these output scan lines proceed to create B-mode US images. Network training loss and validation loss are depicted in Fig.2. Also, an example of a reconstructed signal and its comparison with the ground truth is given in Fig.3.

As apparent from Fig.3, the most noticeable differences between the reference RF signal and the AutoEncoder-reconstructed signal appear in the high-amplitude regions, particularly around the peaks and troughs of the waveform. This suggests that while the AutoEncoder can capture the signal's overall shape and dominant frequency components, it may introduce minor distortion in amplitude and phase. These distortions could arise due to limitations in the model's capacity to precisely encode and reconstruct fine details, mainly when dealing with sharp transitions or high-frequency content. Furthermore, the discrepancies become more evident in the later parts of the signal, where the amplitude diminishes. This could indicate that the model struggles with learning and reconstructing low-amplitude details, possibly due to insufficient training data or the AutoEncoder's inherent bias toward capturing dominant features rather than subtle variations.

Table.2. Comparison of Autoencoder results with conventional methods.

	Nearest	Linear	Spline	Auto-Encoder
SSIM	0.8504	0.8503	0.8383	0.8601
PSNR	17.4511	16.7225	15.9596	17.4129
MS-SSIM	0.7648	0.7482	0.7420	0.7857
FSIM	0.8435	0.8435	0.8389	0.8687
Overal STD	0.2847	0.2826	0.3017	0.2820

Table.2 and Fig.4 demonstrate quantitative and qualitative values and their comparison with conventional methods. The comparative evaluation of reconstruction quality across four methods, Nearest, Linear, Spline, and AutoEncoder, reveals that the AutoEncoder consistently achieves the best overall performance across all image quality metrics. Regarding SSIM, the AutoEncoder yields the highest score of 0.8601, outperforming Nearest 0.8504, Linear 0.8503, and especially Spline 0.8383, indicating superior structural fidelity. Similarly, MS-SSIM and FSIM scores are highest for the AutoEncoder (0.7857 and 0.8687, respectively), suggesting better preservation of multi-scale structural information and feature similarity. While the PSNR of the AutoEncoder 17.4129 dB is slightly lower than that of Nearest 17.4511 dB, the difference is minimal and not substantial enough to offset the consistent improvements seen in other perceptual metrics. Notably, the overall standard deviation (Overall STD) of the AutoEncoder is also the lowest, 0.2820, suggesting more consistent reconstruction performance across the dataset. In contrast, the Spline method yields the lowest metric values across all categories, indicating the weakest performance among the methods evaluated. These results collectively highlight the AutoEncoder's advantage in producing high-fidelity and consistent image reconstructions compared to traditional interpolation techniques.

Also, the visual comparison in Fig.4 further supports these findings, showing that the AutoEncoder reconstructs finer details more effectively than traditional interpolation methods. Overall, the results demonstrate that the AutoEncoder-based approach outperforms interpolation techniques in maintaining structural integrity and feature similarity, making it a promising method for enhancing the lateral resolution of US images.

In addition, Fig.5 presents the Structural Similarity Index (SSIM) performance across 15 reconstructed images using four methods: AutoEncoder, Nearest, Spline, and Linear interpolation. The AutoEncoder method consistently yields higher SSIM scores across most image indices, particularly excelling around indices 4–6 and 9, where the structural differences are more pronounced. This trend suggests that the AutoEncoder is more robust in maintaining structural integrity under varying conditions. The statistical results in the Table further support the comparative performance.3 A paired t-test reveals that the SSIM differences between AutoEncoder and

Spline interpolation are statistically significant (p = 0.0467, t = 2.1815, df = 14), indicating a measurable

IV. DISCUSSION

The results from this study highlight the potential of deep learning-based super-resolution techniques, such as the AutoEncoder, in overcoming the inherent trade-off between lateral and temporal resolution in ultrasound imaging. Traditional methods like nearest, linear, and spline interpolation attempt to enhance lateral resolution by estimating missing spatial information between scan lines. However, their performance is limited in preserving fine structural details. The quantitative evaluation indicates that the AutoEncoder outperforms these interpolation methods across multiple metrics, particularly in SSIM (0.8601) and FSIM (0.8687), which measure structural and feature similarity, respectively. These improvements suggest that the AutoEncoder can reconstruct finer spatial details more effectively while mitigating artifacts and distortions introduced by conventional interpolation techniques.

To statistically validate these differences, paired t-tests were performed comparing the SSIM values of the AutoEncoder to each interpolation method across 15 image pairs. The results showed a statistically significant improvement over the spline method (p = 0.0467, t = 2.1815, df = 14), while differences with nearest (p = 0.9945) and linear (p = 0.2651) interpolation were not statistically significant. These findings confirm that the AutoEncoder provides a measurable advantage over spline interpolation, the poorest-performing method overall, while maintaining at least comparable performance to the other interpolation approaches.

This ability to enhance lateral resolution without requiring additional scan lines presents a significant advantage, as it helps maintain greater spatial detail without the trade-off of reducing frame rate, thus preserving temporal resolution. The relationship between the RF signal reconstruction and image-based results further supports the feasibility of deep learning for ultrasound super-resolution. In the RF domain, the AutoEncoder successfully captured the overall waveform structure. Still, it exhibited slight amplitude and phase deviations, which may contribute to minor errors in the final ultrasound image reconstruction. Despite these minor discrepancies, the method still demonstrated better spatial detail preservation than interpolation techniques. This suggests that the AutoEncoder can learn underlying signal structures effectively, helping to balance lateral resolution enhancement with minimal temporal resolution loss. However, further optimizations, such as training with larger datasets, refining network architectures, or incorporating advanced loss functions tailored for ultrasound imaging, could enhance its ability to generalize across different imaging conditions.

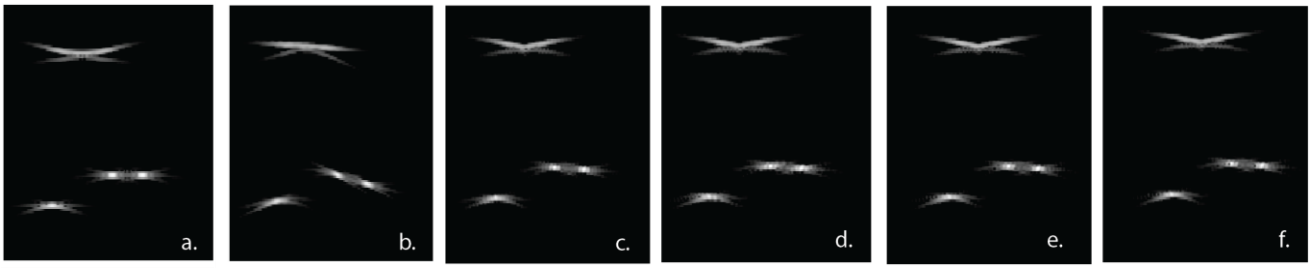

Fig.4. (a) Indicates ground truth (128 scan line). (b) low resolution (64 scan line). (c) results from nearest interpolation. (d) results from linear interpolation. (e) results from spline interpolation. (f) results from Autoencoder.

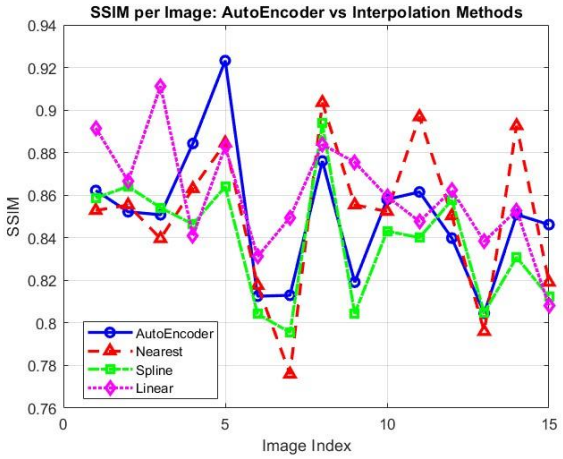

Fig.5. Comparision of SSIM Per-image.

Table.3. Paired t-test results comparing SSIM values of the AutoEncoder method against conventional interpolation methods across 15 images.

	p-Value	t-statistic	df	Significant at $\alpha = 0.05$ level
AutoEncoder-Nearest	0.9945	-0.0070	14	False
AutoEncoder-Spline	0.0467	2.1815	14	True
AutoEncoder-Linear	0.2651	-1.1610	14	False

Improvement in perceptual quality when using the AutoEncoder. In contrast, the differences between AutoEncoder and both Nearest (p = 0.9945) and Linear (p = 0.2651) methods are not statistically significant, suggesting that while the AutoEncoder may visually outperform these approaches in specific images, the overall improvement is not consistent enough to reach statistical significance. Notably, the Nearest method occasionally surpasses the AutoEncoder in specific image indices, but its performance is less stable across the dataset. The plot and statistical analysis demonstrate that the AutoEncoder offers a meaningful improvement over the Spline method and generally delivers competitive or superior SSIM values compared to traditional interpolation methods, highlighting its potential for more perceptually accurate image reconstruction.

V. CONCLUSION

This study demonstrates the effectiveness of an AutoEncoder-based approach in enhancing the lateral resolution of ultrasound images while mitigating the trade-offs associated with traditional interpolation methods. The results indicate that the AutoEncoder outperforms conventional methods in preserving structural details, as evidenced by higher SSIM, MS-SSIM, and FSIM values. The RF signal analysis further supports these findings, showing that while the AutoEncoder captures the general waveform structure, minor deviations in amplitude and phase may contribute to small reconstruction errors in the final image. Despite this, the deep learning-based approach provides a promising alternative to conventional interpolation, offering improved spatial resolution without sacrificing temporal resolution. However, the relatively small dataset size may limit the generalizability of the results to broader clinical scenarios. Additionally, the training process was constrained by computational resources, and a more powerful GPU-equipped system could enable deeper or more complex network architectures and larger batch sizes, potentially leading to improved performance. Future work could focus on refining the model architecture, incorporating larger and more diverse datasets, and optimizing loss functions to enhance performance. These findings highlight the potential of deep learning in overcoming the limitations of traditional ultrasound imaging, paving the way for more accurate and high-resolution diagnostic imaging.

ACKNOWLEDGMENT

This study was supported by the Scientific and Technical Research Council of Turkey (TÜBİTAK) within the scope of the research project under Project Number 122E140.

Authors' Contributions

The authors' contributions to the paper are equal.

Statement of Conflicts of Interest

There is no conflict of interest between the authors.

Statement of Research and Publication Ethics

The authors declare that this study complies with Research and Publication Ethics.

REFERENCES

[1] Bing, X., Zhang, W., Zheng, L., & Zhang, Y. (2019). Medical image super-resolution using improved generative adversarial networks. IEEE Access, 7, 145030-145038.

[2] Housden, R. J., Gee, A. H., Prager, R. W., & Treece, G. M. (2008). Rotational motion in sensorless freehand three-dimensional ultrasound. Ultrasonics, 48(5), 412-422.

[3] Housden, R. J., Treece, G. M., Gee, A. H., & Prager, R. W. (2008). Calibration of an orientation sensor for freehand 3D ultrasound and its use in a hybrid acquisition system. Biomedical engineering online, 7, 1-13.

[4] Nguon, L. S., Seo, J., Seo, K., Han, Y., & Park, S. (2022). Reconstruction for plane-wave ultrasound imaging using a modified U-Net-based beamformer. Computerized Medical Imaging and Graphics, 98, 102073.

[5] Temiz, H., & Bilge, H. S. (2020). Super-resolution of B-mode ultrasound images with deep learning. IEEE Access, 8, 78808-78820.

[6] Mikaeili, M., & Bilge, H. Ş. (2023, November). Evaluating Deep Neural Network Models on Ultrasound Single Image Super Resolution. In 2023 Medical Technologies Congress (TIPTEKNO) (pp. 1-4). IEEE.

[7] van Sloun, R. J., Solomon, O., Bruce, M., Khaing, Z. Z., Wijkstra, H., Eldar, Y. C., & Mischi, M. (2020). Super-resolution ultrasound localization microscopy through deep learning. IEEE transactions on medical imaging, 40(3), 829-839.

[8] Liu, X., Zhou, T., Lu, M., Yang, Y., He, Q., & Luo, J. (2020). Deep learning for ultrasound localization microscopy. IEEE transactions on medical imaging, 39(10), 3064-3078.

[9] Zhang, J., He, Q., Xiao, Y., Zheng, H., Wang, C., & Luo, J. (2021). Ultrasound image reconstruction from plane wave radio-frequency data by a self-supervised deep neural network. Medical Image Analysis, 70, 102018.

[10] Rothlübbers, S., Strohm, H., Eickel, K., Jenne, J., Kuhlen, V., Sinden, D., & Günther, M. (2020, September). Improving image quality of single-plane wave ultrasound via deep learning-based channel compounding. In 2020 IEEE International Ultrasonics Symposium (IUS) (pp. 1-4). IEEE.

[11] Goudarzi, S., & Rivaz, H. (2022). Deep reconstruction of high-quality ultrasound images from raw plane-wave data: A simulation and in vivo study. Ultrasonics, 125, 106778.

[12] Strohm, H., Rothlübbers, S., Eickel, K., & Günther, M. (2020). Deep learning-based reconstruction of ultrasound images from raw channel data. International Journal of Computer Assisted Radiology and Surgery, 15(9), 1487-1490.

[13] Li, Z., Wiacek, A., & Bell, M. A. L. (2020, September). Beamforming with deep learning from single plane wave RF data. In 2020 IEEE International Ultrasonics Symposium (IUS) (pp. 1-4). IEEE.

[14] Hyun, D., Brickson, L. L., Looby, K. T., & Dahl, J. J. (2019). Beamforming and speckle reduction using neural networks. IEEE transactions on ultrasonics, ferroelectrics, and frequency control, 66(5), 898-910.

[15] Wang, Y., Kempski, K., Kang, J. U., & Bell, M. A. L. (2020, September). A conditional adversarial network for single plane wave beamforming. In 2020 IEEE International Ultrasonics Symposium (IUS) (pp. 1-4). IEEE.

[16] Nair, A. A., Tran, T. D., Reiter, A., & Bell, M. A. L. (2018, April). A deep learning-based alternative to beamforming ultrasound images. In 2018 IEEE International Conference on Acoustics, Speech, and Signal Processing (ICASSP) (pp. 3359-3363). IEEE.

[17] Simson, W., Göbl, R., Paschali, M., Krönke, M., Scheidhauer, K., Weber, W., & Navab, N. (2019). End-to-end learning-based ultrasound reconstruction. arXiv preprint arXiv:1904.04696.

[18] Hyun, D., Brickson, L. L., Looby, K. T., & Dahl, J. J. (2019). Beamforming and speckle reduction using neural networks. IEEE transactions on ultrasonics, ferroelectrics, and frequency control, 66(5), 898-910.

[19] Wang, Y., Kempski, K., Kang, J. U., & Bell, M. A. L. (2020, September). A conditional adversarial network for single plane wave beamforming. In 2020 IEEE International Ultrasonics Symposium (IUS) (pp. 1-4). IEEE.

[20] Goudarzi, S., & Rivaz, H. (2022). Deep reconstruction of high-quality ultrasound images from raw plane-wave data: A simulation and in vivo study. Ultrasonics, 125, 106778.

[21] Wasih, M., Ahmad, S., & Almekkawy, M. (2023). A robust cascaded deep neural network for image reconstruction of single-plane wave ultrasound RF data. Ultrasonics, 132, 106981.

[22] https://field-ii.dk/